

Application of CT/MRI Fusion Imaging in the Diagnosis and Staging of Liver Cancer: A Comparative Study

F. Teng, C. Liu, Z. Feng, X. Li*

Department of Radiology, The Second Norman Bethune Hospital of Jilin University, Changchun, 130000, China

ABSTRACT

► Original article

***Corresponding author:**

Xin Li, M.D.,

E-mail:

f18302475018@163.com

Received: September 2023

Final revised: March 2024

Accepted: April 2024

Int. J. Radiat. Res., January 2025;
23(1): 155-161

DOI: 10.61186/ijrr.23.1.155

Keywords: Hepatocellular carcinoma, computed tomography, magnetic resonance imaging, diagnosis, staging.

Background: The purpose of this study is to evaluate the value of computed tomography (CT) / magnetic resonance imaging (MRI) fusion imaging technology in the diagnosis and staging of liver cancer. **Materials and Methods:** Sixty patients with primary hepatocellular carcinoma diagnosed by histopathology and cytology who visited our hospital from April 2021 to May 2023 were selected. All patients underwent CT and MRI single mode scans, as well as CT/MRI fusion imaging scans. Based on the pathological diagnosis results, the consistency and accuracy of three imaging methods in evaluating the number, maximum diameter, and staging of liver cancer patients were compared. **Results:** CT/MRI fusion imaging can more accurately determine the number ($F=8.62$, $P<0.001$), maximum diameter ($F=86.69$, $P<0.001$), and pathological staging of liver cancer lesions compared to single CT or MRI. In terms of determining the number of tumors, CT/MRI fusion imaging is superior to CT (Kappa 0.695 vs 0.654) and MRI (Kappa 0.872 vs 0.695). In terms of evaluating the maximum pathway, CT/MRI fusion imaging has the highest consistency with MRI results (Kappa 0.931), which is significantly better than CT (Kappa=0.818). In staging judgment, CT/MRI fusion imaging improves the diagnostic accuracy of stages II and III tumors.

Conclusion: The CT/MRI fusion imaging technology, which integrates the advantages of CT and MRI imaging examination modes, can improve the display rate, quantitative and staging evaluation accuracy of liver cancer lesions. And it is worthy of further promotion to improve the imaging fine diagnosis level of liver cancer.

INTRODUCTION

Liver cancer remains a global health challenge, with an estimated incidence of over 1 million cases in 2025. Hepatocellular carcinoma (Hepatocellular Carcinoma, HCC) is the most common liver cancer, within 90% of cases (1). Although the diagnosis scheme of liver cancer is being improved, it will still be affected by the accurate diagnosis of factors such as tumor size and number and vascular invasion, resulting in errors in disease diagnosis and prognosis (2). However, most parameters need to make preoperative decision plan based on the results of postoperative pathological examination, especially pathological stage. It can be seen that the timely and accurate diagnosis and reasonable staging of liver cancer need to improve the existing imaging examination methods, so as to improve the accuracy of treatment plan selection and stage judgment.

Imaging is extremely important for the diagnosis of HCC, and the early diagnosis is imperative. Because when the tumor volume of HCC is small, multiple potentially curative treatment options can be obtained for (3). Computed Tomography (CT) and Magnetic Resonance Imaging (MRI) are commonly used imaging modes for evaluating liver cancer (4). Both CT and MRI are suitable for the efficacy

evaluation stage after ultrasound examination in HCC patients (5). CT non-invasive imaging has considerable value for predicting the efficacy in HCC patients after primary TACE (6). Functional MRI techniques, including diffusion-weighted imaging, hepatobiliary contrast agent MRI, perfusion imaging, and magnetic resonance elastography, show promise for providing important information about the biological behavior of tumors (7). However, CT and MRI have their own advantages and disadvantages, and the application of a single mode has certain limitations.

In recent years, a new technology has emerged in the field of medical imaging - image fusion of CT and MRI (8). This technology combines the advantages of CT and MRI imaging modes, and can exert a synergistic effect to improve the sensitivity and specificity of the examination (9). Compared with concurrent use, CT-MRI image fusion method is more accurate in evaluating the edges of ablated lesions and has better predictive value for local tumor progression (10). However, most studies have performed corresponding procedures in liver cancer radiofrequency ablation (11, 12). At present, the application of this new technology for the diagnosis and staging of liver cancer is still relatively rare, and its clinical value needs further confirmation. Therefore, it is necessary to observe the diagnostic

and staging evaluation effects of CT/MRI fusion imaging on liver cancer patients.

This study aims to collect patients with primary hepatocellular carcinoma confirmed by pathological examination, and all patients will undergo CT, MRI single mode scanning, and CT/MRI fusion imaging examination. Evaluate the application prospects of fusion imaging technology in the diagnosis and staging of liver cancer by comparing the effectiveness of three scanning modes in evaluating tumor features. Assuming fusion imaging may improve the detection rate and staging accuracy of liver cancer. This study is the first to apply CT, MRI single mode scanning, and CT/MRI fusion imaging technology to the diagnosis and staging of HCC, and compares the effectiveness of the three scanning modes in evaluating tumor features. Meanwhile, a group of HCC patients confirmed by pathological examination are used, ensuring the accuracy and reliability of the research results. The research assumes that fusion imaging technology may improve the detection rate and staging accuracy of HCC, which will provide a new technical means for imaging examination of HCC patients. This study may provide a new technical means for imaging examination of liver cancer patients.

MATERIALS AND METHODS

General information

Sixty patients diagnosed with primary HCC by histopathology and cytology who visited our hospital from April 2021 to May 2023 were selected. This study has been reviewed and approved by the Medical Ethics Committee of our hospital. Patients inclusion criteria: 1) Confirmed as primary HCC by pathological examination; 2) Imaging examination indicates single or multiple LC; 3) Those who have not undergone radiotherapy or chemotherapy or have undergone hepatic artery chemotherapy/embolization; 4) Accompanied by complete imaging and pathological data; 5) Informed consent and cooperation with various inspections have been obtained, and an informed consent form has been signed. Patients exclusion criteria: 1) Patients with severe dysfunction of important organs such as the heart and lungs; 2) Concomitant severe bleeding tendency or coagulation dysfunction; 3) There are mental disorders or consciousness disorders that affect examination or treatment; 4) Merging secondary LC or having a history of other malignant tumors; 5) Pregnant or lactating women. A total of 38 males and 22 females, aged 41-73 years, with an average age of (58.70 ± 7.00) years, were included. The number of tumors was 1-6, with an average number of (1.68 ± 1.44) . Among them, 41 were single LC, 14 were 2-3 tumors, and 5 were larger than 3 tumors. The maximum diameter of the tumor was

1.20-6.80cm, with an average of (3.56 ± 1.53) cm. 23 cases were less than 3cm, 31 cases were 3-5cm, and 6 cases were more than 5cm. Tumor staging (TNM staging): 12 cases in stage I, 22 cases in stage II, 19 cases in stage III, and 7 cases in stage IV.

Table 1. Patient characteristics.

| Variable | Content | Data |
|-------------------------------------|-------------|------------------|
| Gender | Male | 38 |
| Age (years) | Female | 22 |
| Number of tumors (examples) | | 58.70 ± 7.00 |
| Maximum diameter of tumor (example) | Single shot | 41 |
| TNM staging (example) variable | 2-3 pieces | 14 |
| | >3 | 5 |
| Gender | <3cm | 23 |
| Age (years) | 3-5 cm | 31 |
| Number of tumors (examples) | >5cm | 6 |
| Maximum diameter of tumor (example) | Phase I | 12 |
| TNM staging (example) variable | Phase II | 22 |
| Gender | Phase III | 19 |
| | Phase IV | 7 |

Note: This table is a comprehensive compilation of patient characteristics, TNM: staging criteria for tumor infiltration.

Imaging methods

Instruments and Equipment

CT adopts Philips Brilliance 256 layer iCT (brand: Philips, origin: Netherlands); MRI adopts GE Pioneer 3.0T MRI scanning (brand: GE; origin: United States); CT/MRI image fusion is performed using Velocity AI software (brand: Velocity AI, origin: United States).

(1) CT examination method: The patient is placed in a supine position, with the scanning range starting from the lower edge of sternal stem to the upper pole of kidney, to display the entire liver and part of chest. This method can evaluate the primary lesion and exclude distant organ metastasis. Philips Brilliance 256 layer CT was used, with a tube voltage of 120 kV, a tube current of 250 mAs, a pitch of 0.8, a layer thickness of 5mm, and an interval of 5mm. After the flat scan, a three phase dynamic enhanced scan was performed with the contrast agent Iohexol (total amount 1.5 ml/kg) and an injection rate of 3-5 ml/s. The blood supply and enhancement of the lesion were observed during the arterial phase, portal phase, and delayed phase. (2) MRI examination method: The patient is placed in a supine position. A 3.0T superconducting MRI scanning system (GE Signa HDx) was used, with the head as the first coil. A 16-channel body coil was used for routine scanning (figure 1A). The axial T1 weighted imaging (T1WI) uses a fast multiple echo sequence (FSE): TR 120 ms, TE 4.1 ms, layer thickness 5mm, interval 1 mm, matrix 256×256 . Axial T2 weighted imaging (T2WI) was performed using fast spin echo sequence (FSE): TR 3000ms, TE 80ms, and other parameters were the same as above. Three phases of Gd-DTPA dynamic enhanced scanning were performed, with a contrast agent dose of 0.1 mmol/kg and an injection rate of 2ml/s. Enhanced scans were collected at the arterial

(figure 1B), portal (figure 1C), and delayed stages (13s, 60s, and 180s). Diffusion weighted imaging (DWI) uses single echo EPI sequence (SE-EPI) with b of 0, 800, and 1000 s/mm^2 . Finally, LAVA-Flex sequence scanning was performed to provide lesion specific histological information. Through multi-parameter MRI (figure 1D) examination, the system evaluates the location, signal characteristics, blood supply, and diffusion performance of the lesion, providing information for lesion diagnosis and CT/MRI image fusion. (3) CT/MRI fusion examination method: The digital image data obtained from CT and MRI scans are imported into registration software (MIM) for preprocessing. After cropping, interpolation, and filtering, matching target points are selected between CT/MRI (clear anatomical markers at the bifurcation of liver blood vessels are selected). Automatic rigid body registration of CT and MRI images was achieved using MIM software. Based on the fused images (figure 1E), radiologists performed lesion localization and staging, collected tumor diameter and number, calculated CT values and MRI signals to evaluate tumor staging, and recorded diagnostic results.

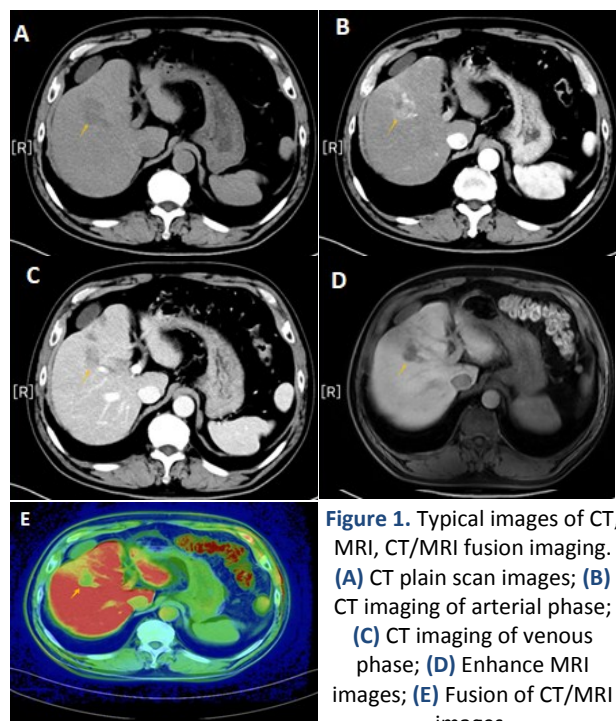


Figure 1. Typical images of CT, MRI, CT/MRI fusion imaging. **(A)** CT plain scan images; **(B)** CT imaging of arterial phase; **(C)** CT imaging of venous phase; **(D)** Enhance MRI images; **(E)** Fusion of CT/MRI images.

Observed indicators

Number of tumors CT examination: Doctors can determine the number of tumors present in the patient's body by scanning the number of images. Each tumor usually appears as an independent nodule or lesion on the scanned image. **MRI examination:** Tumors usually show obvious abnormal areas, which may exhibit different signal characteristics, such as high or low signal. The doctor will mark the location of each tumor and calculate the number of tumors. **CT/MRI fusion examination:**

Doctors will carefully observe the fusion image and search for tumors on the liver or other parts. Each tumor is usually displayed as an independent nodule or lesion on the fusion image, and the number of tumors is understood based on the three-dimensional reconstruction results.

Maximum diameter of tumor CT examination: On the cross-sectional image of the tumor, doctors use measurement tools on the CT image to accurately measure the maximum diameter of the tumor. The maximum path is the distance from the widest point of the tumor to the widest point on the opposite side. **MRI examination:** After locating the tumor, doctors use measurement tools on the MRI image to accurately measure the maximum diameter of the tumor. The maximum path is the distance from the widest point of the tumor to the widest point on the opposite side. **CT/MRI fusion imaging:** On the fusion image, doctors use image measurement tools to accurately measure the maximum diameter of the tumor. The maximum path is the distance from the widest point of the tumor to the widest point on the opposite side.

Tumor staging: Referring to the TNM staging system developed by the International Union for Cancer (UICC) and the American Cancer Society (AJCC) ⁽⁸⁾, TNM staging is defined by imaging doctors. Comprehensive judgments are made based on the patient's tumor location, quantity, tumor diameter, and other factors.

Statistical methods

The statistical software uses SPSS 26.0, the quantitative data is represented by mean \pm standard deviation, and repeated measurement analysis of variance is performed to compare the differences between groups. Pairwise comparison using SNK-q test. Qualitative data is represented by the number of cases and their constituent ratios, and differences between groups are compared using χ^2 test. The consistency rate of tumor maximum diameter measurement, lesion number evaluation, TNM staging and other indicators was calculated, and Kappa test was used to compare the consistency among these three imaging methods. The correction level is $\alpha=0.05$. GraphPad software was used to plot the calculated Kappa test values as variables. Combining the Kappa with SE values, a scatter plot was drawn to clarify the Kappa differences between different test method combinations.

RESULTS

Comparison of examination results for tumors

According to table 2, the detection rate of CT for single tumors was 85.37%, MRI was 95.12%, and CT/MRI fusion was 97.56% ($P>0.05$). The detection rate of CT for 2-3 tumors was 71.43%, MRI was 85.71%,

and CT/MRI fusion was 92.86% ($P>0.05$). Among three tumor groups, the CT detection rate was the lowest at 40.00%, MRI was 60.00%, and CT/MRI fusion was the highest at 100.00% ($P>0.05$). In terms of the average number of tumors, repeated measurement analysis of variance showed significant differences among the three examination methods ($F=8.62$, $P<0.001$). After the LSD-q test, the comparison between CT and CT/MRI fusion was $P=0.001$.

Table 2. Comparison of accurate diagnosis rate and examination results of tumor [Case (%)/Mean±SD].

| Inspection method | Single (n=41) | 2~3 (n=14) | >3 (n=5) | Number of tumors |
|-------------------|---------------|------------|-----------|------------------|
| CT | 35(85.37) | 10(71.43) | 2(40.00) | 1.37±1.29 |
| MRI | 39(95.12) | 12(85.71) | 3(60.00) | 1.58±1.12 |
| CT/MRI fusion | 40(97.56) | 13(92.86) | 5(100.00) | 1.65±1.45 |
| χ^2/F | 5.035 | 2.400 | 4.200 | 8.62 |
| P | 0.081 | 0.301 | 0.123 | <0.001 |

Note: Pairwise comparison, CT and CT/MRI fusion comparison, $P=0.001$; Comparison of MRI and CT/MRI fusion, $P=0.477$; Comparison between CT and MRI, $P=0.435$. CT: CT examination; MRI: MRI examination; CT/MRI fusion: CT/MRI fusion examination; χ^2 : Chi square value; F: Single factor analysis of variance values; P: The difference has a statistically significant threshold. This table compares the diagnostic accuracy of the number of tumors obtained by different examination methods.

Comparison of tumor maximum diameter examination

According to table 3, the detection rate of CT is the lowest for tumors with a maximum diameter of less than 3cm, which is 78.26%. MRI is 95.65%, and CT/MRI fusion is the highest, reaching 100%. The comparison of the three shows $P=0.009$. The detection rate of CT at 3-5 cm was 90.32%, MRI was 96.77%, and CT/MRI fusion was 100% ($P>0.05$). For the maximum diameter > 5cm, the detection rate of these three examination methods was 100% ($P>0.05$). In terms of average maximum diameter, repeated measurement analysis of variance showed significant differences among the three groups ($F=86.69$, $P<0.001$). After the comparison, the pairwise comparison of these three showed $P<0.01$.

Table 3. Tumor diameter detection rate of CT, MRI and CT/MRI fusion.

| Inspection method | <3cm(n=23) | 3~5cm (n=31) | >5cm(n=6) | Maximum diameter of tumor (cm) |
|-------------------|------------|--------------|-----------|--------------------------------|
| CT | 18(78.26) | 28(90.32) | 5(83.33) | 3.93±1.46 |
| MRI | 22(95.65) | 30(96.77) | 6(100.00) | 3.76±1.53 |
| CT/MRI fusion | 23(100.00) | 31(100.00) | 6(100.00) | 3.66±1.53 |
| χ^2/F | 6.845 | 2.882 | 1.588 | 86.69 |
| P | 0.009 | 0.090 | 0.208 | <0.001 |

Note: Pairwise comparison, CT and CT/MRI fusion, $P<0.01$. MRI and CT/MRI fusion, $P<0.01$. CT and MRI, $P<0.01$.

Note: Pairwise comparison, CT and CT/MRI fusion comparison, $P<0.01$; Comparison of MRI and CT/MRI fusion, $P<0.01$; Comparison between CT and MRI, $P<0.01$. CT: CT examination; MRI: MRI examination; CT/MRI fusion: CT/MRI fusion examination; χ^2 : Chi square value; F: Single factor analysis of variance values; P: The difference has a statistically significant threshold. This table compares the accuracy and results of tumor maximum diameter examination obtained by different examination methods.

Comparison of tumor staging examination results

Phase I: The diagnostic accuracy of CT, MRI, and CT/MRI fusion is relatively high, all of which are above 80% ($P>0.05$). Phase II: The accuracy of CT is 81.82%, MRI is 90.91%, and CT/MRI fusion is 100%. The comparison between the three shows $P=0.036$. Phase III: CT has the lowest accuracy of 63.16%, MRI has 78.95%, and CT/MRI fusion has the highest accuracy of 94.74% ($P=0.017$). Phase IV: The accuracy of all three examinations is relatively high, exceeding 70% ($P>0.05$). Overall, the CT/MRI fusion imaging method has improved the accuracy of TNM staging diagnosis for mid-term (II, III) tumors, significantly superior to a single examination.

Table 4. Accuracy comparison of tumor staging examination [Case (%)].

| Inspection method | Phase I (n=12) | Phase II (n=22) | Phase III (n=19) | Phase IV (n=7) |
|-------------------|----------------|-----------------|------------------|----------------|
| CT | 10(83.33) | 18(81.82) | 12(63.16) | 5(71.43) |
| MRI | 11(91.67) | 20(90.91) | 15(78.95) | 6(85.71) |
| CT/MRI fusion | 12(100.00) | 22(100.00) | 18(94.74) | 7(100.00) |
| χ^2 | 2.182 | 4.400 | 5.700 | 2.333 |
| P | 0.140 | 0.036 | 0.017 | 0.127 |

Note: CT: CT examination; MRI: MRI examination; CT/MRI fusion: CT/MRI fusion examination; χ^2 : Chi square value; P: The difference has a statistically significant threshold. This table can reflect the differences in tumor staging accuracy between CT, MRI, and CT/MRI fusion.

Consistency results

The consistency results of these three tests in determining the number of tumors showed lower consistency between CT and MRI ($\text{Kappa}=0.654$), improved consistency between CT and CT/MRI fusion ($\text{Kappa}=0.695$), and the highest consistency between MRI and CT/MRI fusion ($\text{Kappa}=0.872$). In terms of evaluating the maximum diameter of tumors, the consistency of these three examination methods has been improved to varying degrees, especially with the fusion of MRI and CT/MRI achieving very good consistency ($\text{Kappa}=0.931$). In terms of tumor staging judgment, the consistency between CT and MRI was slightly poor ($\text{Kappa}=0.693$), while the consistency between CT/MRI fusion and other single examinations was significantly higher ($\text{Kappa}=0.813-0.852$). Overall, the application of CT/MRI fusion technology can significantly improve the diagnostic consistency with a single CT or MRI, especially in determining the number and staging of tumors in table 5. According to figure 2, the kappa values of these three examination methods for tumor number, maximum tumor diameter, and tumor stage are all higher than 0.60, indicating good consistency among these three.

Table 5. Comparison of Kappa Consistency

| Combination of inspection method | Number of tumors | | Maximum diameter of tumor | | Tumorstaging | |
|----------------------------------|------------------|-------|---------------------------|-------|--------------|-------|
| | Kappa | SE | Kappa | SE | Kappa | SE |
| CT and MRI | 0.654 | 0.085 | 0.693 | 0.069 | 0.693 | 0.069 |
| CT and CT/MRI fusion | 0.695 | 0.080 | 0.818 | 0.016 | 0.813 | 0.053 |
| MRI and CT/MRI fusion | 0.872 | 0.039 | 0.931 | 0.004 | 0.852 | 0.047 |

Note: CT: CT examination; MRI: MRI examination; CT/MRI fusion: CT/MRI fusion examination; χ^2 : Chi square value; P: The difference has a statistically significant threshold. This table can reflect the consistency of tumor staging accuracy between CT, MRI, and CT/MRI fusion.

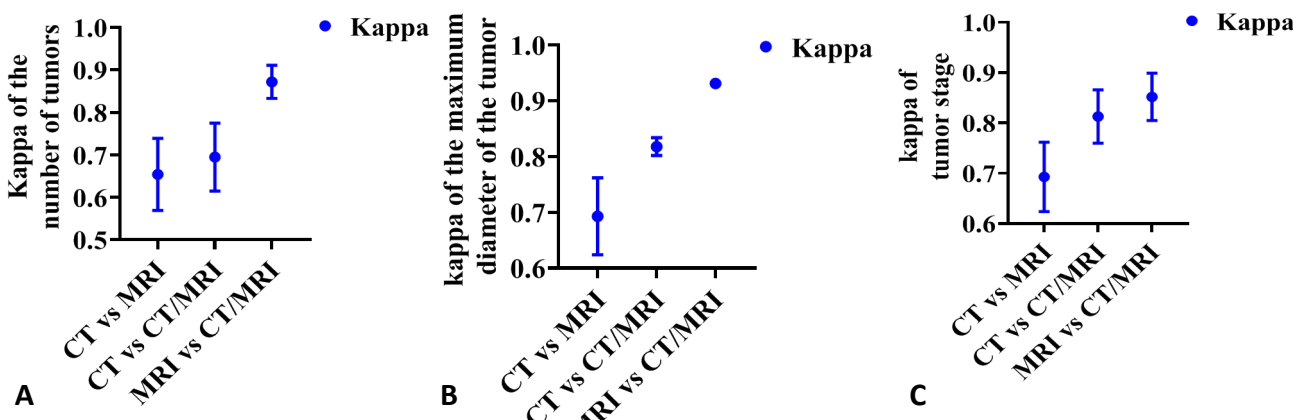


Figure 2. Comparison of Kappa values in CT, MRI, and CT/MRI fusion examinations. **(A)** represents the number of tumors; **(B)** is the maximum diameter of the tumor, and **(C)** is the tumor staging. This figure describes the consistency check differences among three examination methods (CT, MRI, CT/MRI fusion imaging) used for evaluating tumor number, maximum tumor diameter, and tumor staging.

DISCUSSION

In terms of histology, the main subtypes of LC include classical variations, followed by hepatocellular carcinoma with cholangiocarcinoma and fibrous layer variations⁽¹⁴⁾, and are prone to microvascular infiltration⁽¹⁵⁾. These features are easily ignored solely based on a single imaging mode. Fusion imaging integrates CT (which can distinguish the location, shape, and boundary of the tumor⁽¹⁶⁾) and MRI (which is beneficial for identifying microvascular infiltration⁽¹⁷⁾, which can improve the recognition of small lesions⁽¹⁸⁾). In addition, LC has the characteristic of high intrahepatic metastasis, with multiple dynamic changes in the number of lesions. Fusion imaging can depict a comprehensive distribution of lesions⁽¹⁹⁾. Moreover, LC can invade the portal and hepatic veins. Accurately determining the maximum diameter of the lesion and its relationship with blood vessels can better guide surgical procedures and precise tumor resection⁽²⁰⁾. This study shows that CT/MRI fusion imaging has the characteristic of accurately determining the key parameters of LC lesions compared to CT or MRI imaging alone. This is closely related to the pathological and physiological characteristics of LC. Therefore, theoretically speaking, CT/MRI fusion imaging technology has a higher degree of compatibility with the biological behavior of LC, and can improve the accuracy of lesion detection and quantitative evaluation.

CT/MRI fusion imaging is a medical image fusion technology based on wavelet packet transform

theory. This technology first performs wavelet packet transform on CT and MRI images to extract low-frequency and high-frequency information of the two mode images. Then, electronic adaptive medical operators are used to fuse the low-frequency information of the two images to obtain the approximate coefficients of the fused images. Finally, the high-frequency information of the two images is used as the detailed coefficients of the fused image, and the fused image is subjected to inverse wavelet packet transform to obtain the fused images of CT and MRI⁽²¹⁾. The advantage of this technology is that it can improve the detection rate of early LC lesions smaller than 2cm, enabling more single lesions to be detected and treated in a timely manner, and improving prognosis⁽²²⁾. And it can more accurately measure the size and number of lesions, providing more accurate imaging basis for TNM staging and surgical selection. It can also clearly determine the spatial relationship between tumors and blood vessels, guiding surgeons to develop personalized tumor resection and liver reconstruction plans⁽²³⁾. Therefore, the application of CT/MRI fusion imaging will optimize the diagnosis and treatment process of LC, and effectively improve the quality of life of patients. This technology is worth promoting and applying in clinical practice to further improve the therapeutic effect of LC.

The results of this study show that CT/MRI fusion imaging can more accurately determine the number, maximum diameter, and pathological staging of liver cancer lesions compared to single CT or MRI. CT/MRI fusion imaging is superior to CT and MRI in

determining the number of tumors. In terms of evaluating the maximum path, CT/MRI fusion imaging has the highest consistency with MRI results, which is significantly better than CT. Ayuso *et al.* (24) also found that CT/MRI fusion imaging is more accurate in determining the number and maximum diameter of liver cancer lesions compared to simple CT or MRI. A new method for calculating 3D activity and ITV potential of liver cancer using MRI has achieved accurate calculation of respiratory activity of mobile structures (25). CT/MRI fusion imaging evaluation is not easily affected by patient breathing, especially suitable for patients with unsatisfactory 4DCT imaging (26). 4D-MRI reconstruction may result in severe or slight artifacts, mainly due to irregular activity during image acquisition (27). CT/MRI image fusion volume navigation can clearly locate and diagnose liver lesions in patients with primary liver cancer or metastatic diseases (28). Xu *et al.* (29) found that CT/MRI fusion imaging is superior to a single imaging mode in assessing the therapeutic response of liver cancer to thermal ablation, but the number, size, and staging of lesions were not observed. In staging determination, CT/MRI fusion imaging has improved the diagnostic accuracy of stage II and III tumors. This is consistent with the research findings of Lima *et al.* (30), who found that CT/MRI fusion imaging can improve the detection rate of early liver cancer and reduce it. However, this study also has certain limitations as the sample size is small and requires further validation. In addition, the standardized operation and interpretation of image fusion also need to establish expert consensus.

CONCLUSION

In summary, CT/MRI fusion imaging technology, which integrates the advantages of CT and MRI imaging examination modes, can improve the display rate, quantitative and staging evaluation accuracy of liver cancer lesions, and is worth further promotion to enhance the level of imaging fine diagnosis of liver cancer. It can be considered that CT/MRI fusion imaging technology can significantly improve the imaging diagnosis level of liver cancer, and its application prospects in liver cancer screening and precision surgery are broad.

ACKNOWLEDGMENT

None.

Funding: None.

Conflict of interests: The authors declare no conflict of interests.

Ethical approval: This article does not contain any studies with human participants performed by any of the authors.

Authors Contribution: F.T., research experiments;

C.L., data analysis; Z.F. and X.L. helped with the constructive discussion; F.T., C.L., Z.F., X.L., manuscript preparation and final approval.

REFERENCES

1. Llovet JM KRK, Villanueva A *et al.* (2021) Hepatocellular carcinoma. *Nature Reviews Disease Primers*, **7**(1): 6.
2. Gong XQ TYY, Wu YK *et al.* (2021) Progress of MRI radiomics in hepatocellular carcinoma. *Front Oncol*, **11**: 698373.
3. Hennedige T and Venkatesh SK (2016) Advances in computed tomography and magnetic resonance imaging of hepatocellular carcinoma. *World J Gastroenterol*, **22**(1): 205-20.
4. Chartampilas ERV, Georgopoulou VKG, Hatzidakis APP (2022) Current imaging diagnosis of hepatocellular carcinoma. *Cancers (Basel)*, **14**(16): 3997.
5. Dalla Palma L and Pozzi-Mucelli RS (1992) Computed tomography and magnetic resonance imaging in diagnosing hepatocellular carcinoma. *Ital J Gastroenterol*, **24**(2): 87-91.
6. Dai Y, Liu D, Xin Y, *et al.* (2023) Efficacy and interpretability analysis of noninvasive imaging based on computed tomography in patients with hepatocellular carcinoma after initial transarterial chemoembolization. *Acad Radiol*, **30** (Suppl 1): S61-S72.
7. Jiang HY, Chen J, Xia CC, Cao LK, Duan T, Song B (2018) Noninvasive imaging of hepatocellular carcinoma: From diagnosis to prognosis. *World J Gastroenterol*, **24**(22): 2348-2362.
8. Fang D YC, Zhou H, *et al.* (2022) Effects of CT/MRI image fusion on cerebrovascular protection, postoperative complications, and limb functional recovery in patients with anterior and middle skull -base tumors: Based on a retrospective cohort study. *Contrast Media Mol Imaging*, **2022**: 785576.
9. Chen C XLC, Wang Y, *et al.* (2019) Assessment of the cryoablation margin using MRI-CT fusion imaging in hepatic malignancies. *Clin Radiol*, **74**(8): 652.e21-652.e28.
10. Zhou H, Yang G, Jing X, *et al.* (2023) Predictive value of ablative margin assessment after microwave ablation for local tumor progression in medium and large hepatocellular carcinoma: Computed tomography-computed tomography image fusion method versus side-by-side method. *J Comput Assist Tomogr*, **47**(1): 31-37.
11. Yi JS CG (2022) Application of ultrasound fusion imaging in thermal ablation of large hepatocellular carcinoma. *Modern Medical Imagingology*, **31**(12): 2322-2324.
12. Lan SR-XJW and Zhang YM-EA (2022) Guidance of real-time contrast-enhanced ultrasonography and 3D ultrasound fusion imaging for ablation area in patients with primary liver cancer during microwave ablation therapy. *Journal of Practical Hepatology*, **25**(6): 889-892.
13. Kuo KL, Stenehjem D, Albright F, Ray S, Brixner D (2015) Treatment patterns and outcomes in patients with hepatocellular carcinoma stratified by stage-guided treatment categories. *J Natl Compr Canc Netw*, **13**(8): 987-94.
14. Hui M, Uppin SG, Uppin MS, *et al.* (2023) Hepatocellular carcinoma: A clinicopathological and immunohistochemical study of 116 cases from a tertiary care hospital in Southern India. *Indian J Cancer*, **60**(2): 191-198.
15. Zhu Y, Feng B, Cai W, *et al.* (2023) Prediction of microvascular invasion in solitary AFP-negative hepatocellular carcinoma ≤ 5 cm using a combination of imaging features and quantitative dual-layer spectral-detector CT parameters. *Academic Radiology*, **(23)**: 1076-1032.
16. Chen L, Ruan S, Wang P, *et al.* (2023) Imaging features of primary hepatic sarcomatoid carcinoma: Differentiation from hepatocellular carcinoma and intrahepatic cholangiocarcinoma on CT: A preliminary study. *Helicon*, **9**(3): e14123.
17. Cha DI, Kang TW, Jeong WK, Kim JM, Choi GS, Joh JW, Yi NJ, Ahn SH (2024) Preoperative assessment of microvascular invasion risk using gadoxetate-enhanced MRI for predicting outcomes after liver transplantation for single hepatocellular carcinoma within the Milan criteria. *Eur Radiol*, **34**(1): 498-508.
18. Makino Y, Imai Y, Igura T, *et al.* (2012) Usefulness of the multimodality fusion imaging for the diagnosis and treatment of hepatocellular carcinoma. *Dig Dis*, **30**(6): 580-7.
19. Dong Y, Wang WP, Mao F, Ji ZB, Huang BJ (2016) Application of imaging fusion combining contrast-enhanced ultrasound and magnetic resonance imaging in detection of hepatic cellular carci-

nomas undetectable by conventional ultrasound. *J Gastroenterol Hepatol*, **31**(4): 822-8.

20. Uraki J YK and Nakatsuka A TK (2004) Transcatheter hepatic arterial chemoembolization for hepatocellular carcinoma invading the portal veins: therapeutic effects and prognostic factors. *Eur J Radiol*, **51**(1): 12-18.

21. Wang L LB and Tian LF (2014) Multi-modal medical image fusion using the inter-scale and intra-scale dependencies between image shift-invariant shearlet coefficients. *Information Fusion*, **19**: 20-28.

22. Wu W JX, Xue GQ, et al. (2022) A multicenter randomized controlled study of contrast-enhanced US versus US-guided biopsy of focal liver lesions. *Radiology*, **305**(3): 721-728.

23. Zhang EL CQ and Huang ZY DW (2021) Revisiting surgical strategies for hepatocellular carcinoma with microvascular invasion. *Front Oncol*, **11**: 691354.

24. Ayuso C RJ, Vilana R, et al. (2018) Diagnosis and staging of hepatocellular carcinoma (HCC): current guidelines. *Eur J Radiol*, **101**(5): 72-81.

25. Akino Y, Oh RJ, Masai N, Shiomi H, Inoue T (2014) Evaluation of potential internal target volume of liver tumors using cine-MRI. *Med Phys*, **41**(11): 111704.

26. Fernandes AT, Apisarthanarax S, Yin L, et al. (2015) Comparative assessment of liver tumor motion using cine-magnetic resonance imaging versus 4-dimensional computed tomography. *Int J Radiat Oncol Biol Phys*, **91**(5): 1034-40.

27. Yang J, Wang H, Yin Y, Li D (2015) Retracted: Reducing motion artifacts in 4D MR images using principal component analysis (PCA) combined with linear polynomial fitting model. *J Appl Clin Med Phys*, **16**(2): 5165.

28. Rennert J, Georgieva M, Schreyer AG, et al. (2011) Image fusion of contrast enhanced ultrasound (CEUS) with computed tomography (CT) or magnetic resonance imaging (MRI) using volume navigation for detection, characterization and planning of therapeutic interventions of liver tumors. *Clin Hemorheol Microcirc*, **49**(1-4): 67-81.

29. Xu E LY and Li K EA (2019) Comparison of CT/MRI-CEUS and US-CEUS fusion imaging techniques in the assessment of the thermal ablation of liver tumors. *Int J Hyperthermia*, **35**(1): 159-167.

30. Lima PH FB, Bérubé J, et al. (2019) Cost-utility analysis of imaging for surveillance and diagnosis of hepatocellular carcinoma. *Am J Roentgen*, **213**(1): 17-25.

